

# Quasimonoenergetic and low emittance ion bunch generation from ultrathin targets by counterpropagating laser pulses of ultrarelativistic intensities

H.K. Avetissian,\* A.K. Avetissian, G.F. Mkrtchian, and Kh.V. Sedrakian

*Centre of Strong Fields Physics, Yerevan State University, 1 A. Manukian, Yerevan 0025, Armenia*

(Dated: July 29, 2018)

A new method for generation of quasimonoenergetic and low emittance fast ion/nuclei bunches of solid densities from nanotargets by two counterpropagating laser pulses of ultrarelativistic intensities is proposed, based on the threshold phenomenon of particles "reflection" due to induced nonlinear Compton scattering. Particularly, a setup is considered which provides generation of ion bunches with parameters that are required in hadron therapy.

PACS numbers: 41.75.Jv, 52.38.Kd, 37.10.Vz, 52.65.Rr

Acceleration of ions with superstrong laser beams has attracted broad interest over the last years conditioned by a number of important applications, such as inertial confinement fusion [1], isotope production [2], hadron therapy [3], and etc. Most of these mechanisms are based on the indirect processes, when ions are accelerated by the space-charge fields induced in the laser-target interaction process. There are several regimes of ions acceleration depending on the laser intensity: Target Normal Sheath Acceleration regime [4], Coulomb Explosion regime [5], Radiation Pressure Dominant regime [6], and the shock wave acceleration mechanism [7]. Typically in Target Normal Sheath Acceleration regime, the accelerating gradient reaches of  $10^{12}$  V/m, but due to short interaction range  $\sim 1 \mu\text{m}$  it accelerates the ions to tens of MeV energies. The energy distribution of accelerated ions obtained by the laser plasma interaction is usually exponential with almost 100% energy spread up to a cutoff energy. Only within the last years became possible to produce monoenergetic ion beams from targets using special technique [8]. In these experiments up to 60 MeV protons was observed. In Radiation Pressure Dominant regime, with circularly polarized laser pulses when heating of electrons is reduced, it is expected to achieve GeV/nucleon energy range at the ultrarelativistic laser intensities [9].

The use of mentioned indirect processes for ions acceleration, because of the lack of directly accelerating laser fields of required intensities, has some undesirable factors, such as uncontrollable beam parameters, etc. The state-of-the-art laser systems are capable of generating electromagnetic pulses with intensities exceeding on several orders the threshold of relativism for electrons. For heavy particles, laser intensities, at which, e.g., an ion with atomic mass number  $\mathcal{A}$  and charge number  $\mathcal{Z}$  becomes relativistic, is defined by the condition  $\Xi \gtrsim 1$ , where  $\Xi = \mathcal{Z}eE\lambda/\mathcal{A}m_u c^2$  is relativistic dimensionless parameter of a wave-particle interaction ( $e$  is the elementary charge,  $c$  is the light speed in vacuum, and  $m_u$  is the atomic mass unit  $m_u \simeq 1.66 \times 10^{-24}$  g) and represents the work of the field with electric strength  $E$  on a wavelength  $\lambda$  ( $\tilde{\lambda} = \lambda/2\pi$ ) in the units of particle rest energy.

Laser intensities, at which relativistic effects become important for an ion ( $\Xi = 1$  -threshold value) can be estimated as:  $I_r = \mathcal{A}^2 \mathcal{Z}^{-2} \times 4.55 \times 10^{24} \text{ W cm}^{-2} [\lambda/\mu\text{m}]^{-2}$ . The availability of such intensities now is in the scope of ELI project [10] and it is of interest the mechanisms for direct laser acceleration of heavy particles. The spectrum of direct acceleration mechanisms of nuclei/ions by a single laser pulse is very restricted, since one should use the laser beams focused to subwavelength waist radii, or use subcycle laser pulses. Direct acceleration of ions by petawatt laser beams focused to subwavelength waist radii has been explored with radially polarized lasers [11], where ions energies cover the domain of application in hadron therapy [3]. However, the realization of this scheme with radially polarized laser pulses of required ultrarelativistic intensities is problematic. Hence, it is reasonable (for low energy spreads and emittances of accelerated ions bunches) to consider coherent processes of laser-particle interaction. Among those induced Compton process is practically more effective. Thus, in this process a critical value of intensity exists [12] above which the nonlinear threshold phenomenon of particles "reflection" occurs from the formed moving wave-barrier which opens a principally new way for particles acceleration on the short distances -even shorter than a wavelength [13]. Note, however, that this phenomenon of critical field, in principle, takes place for plane waves. How the critical-field-effect will change the interaction dynamics for strongly nonplane -tightly focused ultrarelativistic laser pulses, this is a problem for investigation in an each specific case, for concrete pulse-configurations (see, e.g. [14]).

In this letter we propose a new method for generation of solid density, monoenergetic and low emittance ions/nuclei bunches of ultrashort durations. Accordingly, we will study laser acceleration of ions/nuclei in the induced Compton process with strongly nonplane ultrashort pulses, taking into account the specific feature of the critical field for generation of fast ion beams with low energy spreads and emittances. For realization of the latter we propose to focus two counterpropagating laser beams of different frequencies and ultrarel-

ativistic intensities onto an nanoscale-solid-plasma targets with  $\mathcal{Z}/\mathcal{A} = 1; 1/2$  (for protons and nuclei, respectively). In particular, we consider the specific range of energies that is of great interest to hadron therapy [3] with quasimonoenergetic-monochromatic ion beams.

At first we consider the classical dynamics of an ion in vacuum at the interaction with two counterpropagating plane waves of carrier frequencies  $\omega_1, \omega_2$  (let  $\omega_1 > \omega_2$ ), wavenumbers  $\mathbf{k}_1 = \{\omega_1/c, 0, 0\}$ ,  $\mathbf{k}_2 = \{-\omega_2/c, 0, 0\}$ , and slowly varying electric field amplitudes  $E_1(\tau_1), E_2(\tau_2)$  ( $\tau_1 = t - x/c, \tau_2 = t + x/c$ ). Both waves are assumed to be linearly polarized along the  $OY$  direction:

$$\mathbf{E}_{1,2}(x, t) = \{0, E_{1,2}(\tau_{1,2}) \cos \omega_{1,2}\tau_{1,2}, 0\}. \quad (1)$$

Dynamics of an ion in the resulting electric  $\mathbf{E} = \mathbf{E}_1 + \mathbf{E}_2$  and magnetic  $\mathbf{H} = \hat{\mathbf{x}} \times (\mathbf{E}_1 - \mathbf{E}_2)$  fields is governed by the equations:

$$\frac{d\mathbf{\Pi}}{dt} = \frac{e\mathcal{Z}}{\mathcal{A}m_u c} \left( \mathbf{E} + \frac{\mathbf{\Pi} \times \mathbf{H}}{\gamma} \right), \quad \frac{d\gamma}{dt} = \frac{e\mathcal{Z}}{\mathcal{A}m_u c} \frac{\mathbf{\Pi} \cdot \mathbf{E}}{\gamma}. \quad (2)$$

Here we have introduced normalized momentum  $\mathbf{\Pi} = \mathbf{p}/(\mathcal{A}m_u c)$  and energy  $\gamma = \sqrt{1 + \mathbf{\Pi}^2}$  (Lorentz factor). When the particle initial transversal momentum is zero, and the waves are turned on/off adiabatically at  $t \rightarrow \mp\infty$ , from Eq. (2) for transversal momentum one can obtain (coordinate  $z$  is cyclic, so  $\Pi_z = \text{const} \equiv 0$ ):

$$\Pi_y(\Xi_1, \Xi_2) = \Xi_1(\tau_1) \sin \omega_1 \tau_1 + \Xi_2(\tau_2) \sin \omega_2 \tau_2. \quad (3)$$

With the help of Eq. (3), one can obtain equations for longitudinal momentum and energy, which include four nonlinear interaction terms: two of them are proportional to  $\Xi_{1,2}^2(\tau_{1,2}) \sin 2\omega_{1,2}\tau_{1,2}$  and describe interaction with separate waves that can not provide real energy change for ion. The term proportional to  $\Xi_1(\tau_1) \Xi_2(\tau_2) \sin(\omega_1\tau_1 + \omega_2\tau_2)$  describes interaction with the fast interference wave making no contribution to real energy exchange too. This term is responsible for particle-antiparticle pair production from Dirac vacuum [15]. The resonant interaction of the ion for acceleration is governed by the slowed interference wave  $\Xi_1(\tau_1) \Xi_2(\tau_2) \sin \tilde{\omega}(t - x/c\beta_{ph})$ , where  $\tilde{\omega} = \omega_1 - \omega_2$  and  $\beta_{ph} = \tilde{\omega}/(\omega_1 + \omega_2) < 1$  are the frequency and phase velocity of the slowed wave. Hence, keeping only this resonant term, one can obtain the following integral of motion in average:

$$\gamma - \beta_{ph}\Pi_x \simeq \gamma_0 - \beta_{ph}\Pi_{0x}. \quad (4)$$

From Eqs. (4), (3) and dispersion relation  $\gamma = \sqrt{1 + \mathbf{\Pi}^2}$  one can see that for the certain values of  $\Xi_{1,2}$  (which we call critical) the following relation for an ion average transversal momentum in the field may be satisfied:

$$\sqrt{\Pi_y^2(\Xi_1, \Xi_2)} > \gamma_0 |\beta_{ph} - \beta_{0x}| (1 - \beta_{ph}^2)^{-1/2},$$

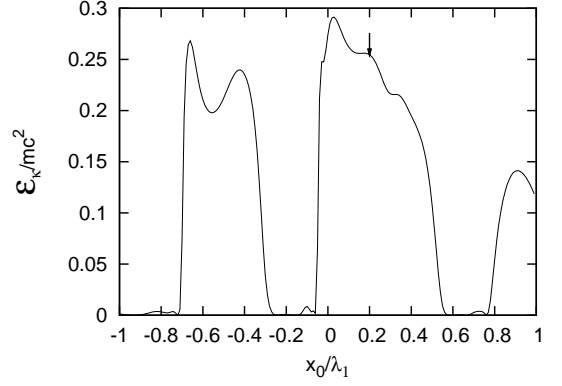


FIG. 1: The final scaled kinetic energy versus the initial position of the ion  $x_0$  in units of wavelength  $\lambda_1$ . The arrow shows the position of the target layer.

at which the slowed interference wave becomes a potential barrier causing ion reflection from this moving wave-barrier. After the interaction ( $\Xi_{1,2} = 0$ ) for the reflected ion final energy we have:

$$\gamma_f \simeq \gamma_0 + 2\gamma_0\beta_{ph}(\beta_{ph} - \beta_{0x})(1 - \beta_{ph}^2)^{-1}. \quad (5)$$

Formula (5) shows that ion acceleration depends neither on the fields' magnitudes nor the interaction length. Namely this feature of reflection phenomenon is used here for generation of monoenergetic and low emittance ions/nuclei bunches of ultrashort durations.

Then for actual strongly nonplane and supershort ultrarelativistic laser pulses of certain configurations the problem is solved with the help of particle-in-cell (PIC) simulations. Here we report on the results of the 2D3V PIC simulations of counterpropagating waves interaction with nanolayers. We use the code XOOPIC, which is a relativistic code based on PIC method [16]. Then we consider two type of ion targets: ionized hydrogen  $^1\text{H}^+$  and fully ionized carbon  $^{12}\text{C}^{6+}$ . The simulation box size is  $40\lambda_1 \times 20\lambda_1$  in  $xy$  plane. Number of cells are  $4000 \times 200$ . The total number of macro-particles is about  $4 \times 10^4$  for hydrogen target and  $2.4 \times 10^5$  -for carbon target. Target is assumed to be fully ionized. This is justified since the intensity for fully ionization of carbon is about  $10^{19}$   $\text{W}/\text{cm}^2$ , while we use in simulations intensities at least on five orders of magnitude larger. So, the target will become fully ionized well before the arrival of the pulses' peaks. Electrons and ions are assumed to be cold in the target,  $T_e = T_i = 0$ .

The laser pulses have profiles  $\sin^2(\pi t/\mathcal{T}_{1,2})$  with pulse durations  $\mathcal{T}_1 = 5\lambda_1/c, \mathcal{T}_2 = 3\lambda_2/c$  and Gaussian transverse profiles:  $\exp(-r^2/w_{1,2}^2)$ , with the waists  $w_1 = 6\lambda_1$  and  $w_2 = 3\lambda_2$ . The carrier-envelope-phase of the lasers is set to zero, so that the electric fields' maximums are at the pulses' centers. The first laser ( $\omega_1$ ) is introduced at the left boundary and propagates along the  $x$  axis

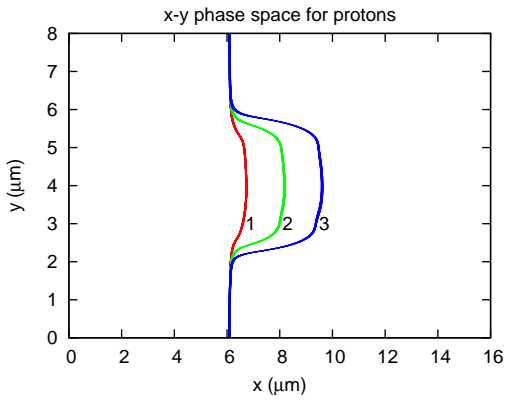


FIG. 2: (Color online) Ion layer blown out from a thin foil by counter-propagating waves. The  $(x - y)$  phase space for protons at instants (1)  $15T_2$ , (2)  $18T_2$  and (3)  $21T_2$ .

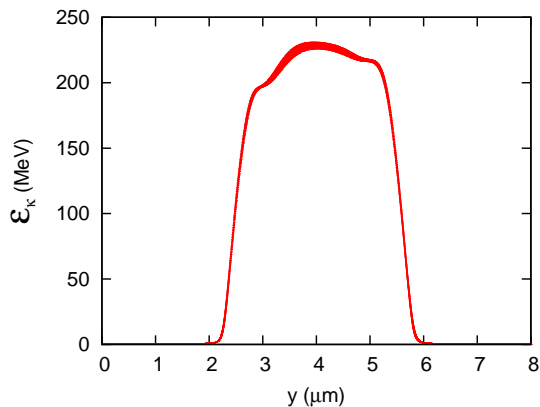


FIG. 3: (Color online) The final kinetic energy distribution (at instant  $21T_2$ ) of accelerated protons versus the transversal position  $y$ .

from left to right, is focused at the target layer. The second laser ( $\omega_2$ ) is introduced at the right boundary and is also focused at the target layer. We consider case  $\lambda_1 = \lambda_2/2$  when  $\lambda_2 = 800$  nm which for the phase velocity of the slowed wave gives:  $\beta_{ph} = 1/3$  and according to Eq. ((5)) for reflected particle normalized kinetic energy gives:  $\gamma_f - 1 \approx 0.25$ . Before PIC simulation we have cleared up the role of initial conditions. It is evident that for the short laser pulses, depending on the initial position of an ion, reflection will take place with various longitudinal velocities (acquired in the fields), resulting to different final energies. This is well seen from Fig. 1, displaying the role of initial conditions: the final energy versus the initial position  $x_0$  of an ion for plane waves, at  $\mathbf{v}_0 = 0$ . The intensity of effective slowed wave is above the critical point:  $\Xi_1 = 0.6$ ,  $\Xi_2 = 0.3$ . Numerical results show that this model is almost accurate in predicting the final energies of reflected particles. Thus, taking into account the result for PIC simulations, the target layer is placed at the distance of  $15.2\lambda_1$  from the left boundary,

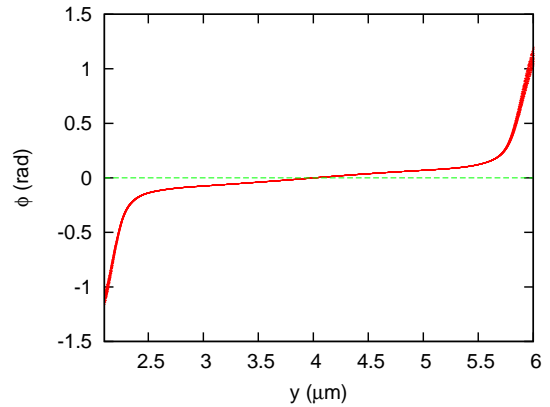


FIG. 4: (Color online) The angular distribution of accelerated protons versus the transversal position  $y$ .

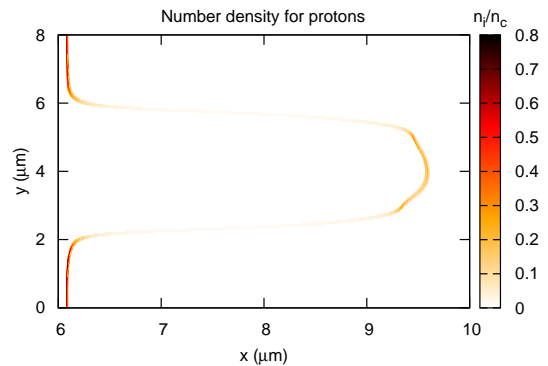


FIG. 5: (Color online) Density distribution of protons at instant  $21T_2$ .

and the first laser is introduced with time delay to start pulse:  $t_{del} = 10\lambda_1/c$ .

In Fig. 2 ion layer blown out from a thin  $^1\text{H}^+$  target of thickness 8 nm by counter-propagating waves, is shown for various instants. Here  $n_e = n_c$ , where as a measure of density we take critical plasma density  $n_c = 1.74 \times 10^{21} \text{ cm}^{-3}$  calculated for 800 nm laser. Note that electrons are escaped from the target before the arrival of the pulses' peaks. At the  $21T_2$  the ions are already free. The final kinetic energy  $\mathcal{E}_k$  and angular  $\phi = \tan^{-1}(\Pi_x/\Pi_y)$  distributions of accelerated protons versus the transversal position, are shown in Figs. 3 and 4, respectively. The number density of protons is displayed in Fig. 5. The results for carbon foil of density  $n_e = 80n_c$  and 4 nm thickness are shown in Figs. 6, 7, 8. Estimates for transverse ( $\epsilon_t$ ) and longitudinal ( $\epsilon_l$ ) emittances of the ions bunch show that for protons  $\epsilon_t < 0.1\pi$  mm mrad and  $\epsilon_l < 10^{-8}$  eV s, while for carbon ions  $\epsilon_t < 0.1\pi$  mm mrad and  $\epsilon_l < 10^{-7}$  eV s. These results are on several orders of magnitude smaller than their counterparts in conventional ion accelerators. The

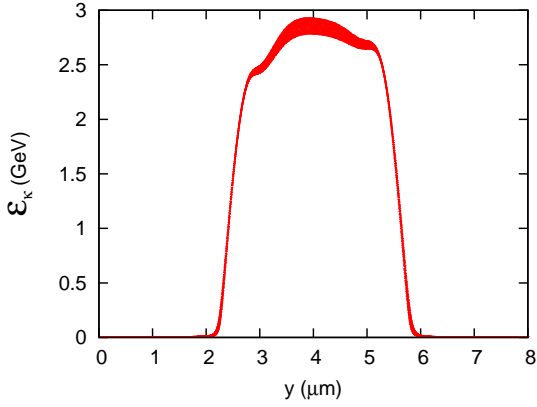


FIG. 6: (Color online) The final kinetic energy distribution of carbon ions versus the transversal position  $y$ .

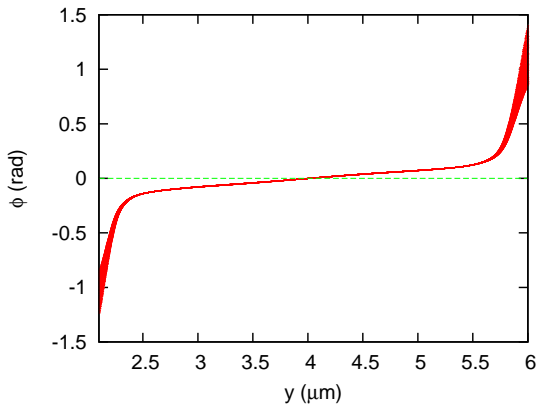


FIG. 7: (Color online) The angular distribution of accelerated carbon ions versus the transversal position  $y$ .

energy spreads are:  $\delta\mathcal{E}/\mathcal{E} \sim 10^{-2}$ .

In conclusion, owing to the threshold character of particle reflection phenomenon, efficient generation of quasi-monoenergetic and low emittance fast ion bunches of solid densities from nanotargets by counterpropagating laser pulses of ultrarelativistic intensities has been put forward and demonstrated with PIC simulations. Particularly, a setup is considered which provides generation of ion bunches in the range of such energies and low spreads that may have application in hadron therapy.

This work was supported by SCS of RA.

\* Electronic address: avetissian@ysu.am

- [1] M. Roth *et al.*, Phys. Rev. Lett. **86**, 436 (2001); A. Macchi *et al.*, Nucl. Fusion **43**, 362 (2003); M. Temporal, J. J. Honrubia, S. Atzeni, Phys. Plasmas **15**, 052702 (2008); J.J. Honrubia *et al.*, *ibid.* **16**, 102701 (2009); N. Naumova *et al.*, Phys. Rev. Lett. **102**, 025002 (2009).  
 [2] S. Fritzler *et al.*, Appl. Phys. Lett. **83**, 3039 (2003); E.

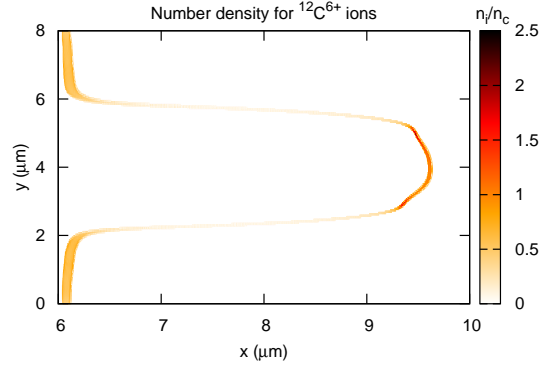


FIG. 8: (Color online) Density distribution for carbon ions at instant  $21T_2$ .

- Lefebvre *et al.*, J. Appl. Phys. **100**, 113308 (2006).  
 [3] E. Fourkal *et al.*, Med. Phys. **29**, 2788 (2002); V. Malka *et al.*, Med. Phys. **31**, 1587 (2004); S. S. Bulanov *et al.*, *ibid.* **35**, 1770 (2008); I. Hofmann, J. Meyer-ter-Vehn, X. Yan, A. Orzhekhovskaya, S. Yaramyshev Phys. Rev. ST AB **14**, 031304 (2011).  
 [4] S.C. Wilks *et al.*, Phys. Plasmas **8**, 542 (2001); T.Z. Esirkepov *et al.*, Phys. Rev. Lett. **89**, 175003 (2002); H. B. Zhuo *et al.*, *ibid.* **105**, 065003 (2010).  
 [5] S.V. Bulanov *et al.*, Phys. Lett. A **299**, 240 (2002); E. Fourkal, I. Velchev, C.-M. Ma, Phys. Rev. E **71**, 036412 (2005); S. S. Bulanov *et al.*, *ibid.* **78**, 026412 (2008).  
 [6] T. Esirkepov, M. Borghesi, S.V. Bulanov, G. Mourou, T. Tajima, Phys. Rev. Lett. **92**, 175003 (2004); S.G. Rykovanov *et al.*, New J. Phys. **10**, 113005 (2008); A.A. Gonoskov, A.V. Korzhimanov, V.I. Eremin, A.V. Kim, A.M. Sergeev, Phys. Rev. Lett. **102**, 184801 (2009); S.V. Bulanov *et al.*, *ibid.* **104**, 135003 (2010).  
 [7] L. O. Silva *et al.*, Phys. Rev. Lett. **92**, 015002 (2004).  
 [8] S. Ter-Avetisyan *et al.*, Phys. Rev. Lett. **96**, 145006 (2006); B. M. Hegelich *et al.*, Nature **439**, 441 (2006); H. Schwöerer *et al.*, Nature **439**, 445 (2006).  
 [9] A. Macchi, F. Cattani, T.V. Liseykina, F. Cornolti, Phys. Rev. Lett. **94**, 165003 (2005); A. Macchi, S. Veghini, F. Pegoraro, *ibid.* **103**, 085003 (2009); X.Q. Yan, H.C. Wu, Z.M. Sheng, J.E. Chen, J. Meyer-ter-Vehn, *ibid.* **103**, 135001 (2009); A. Henig *et al.*, *ibid.* **103**, 245003 (2009).  
 [10] The Extreme Light Infrastructure (ELI) project: [www.extreme-light-infrastructure.eu/eli-home.php](http://www.extreme-light-infrastructure.eu/eli-home.php)  
 [11] Y.I. Salamin, Z. Harman, C.H. Keitel, Phys. Rev. Lett. **100**, 155004 (2008).  
 [12] V.M. Haroutunian, H.K. Avetissian, Phys. Lett. A **59**, 115 (1976).  
 [13] H.K. Avetissian, *Relativistic Nonlinear Electrodynamics* (Springer, New York, 2006).  
 [14] H.K. Avetissian, Kh.V. Sedrakian, Phys. Rev. ST AB **13**, 101304 (2010); *ibid.* **13**, 081301 (2010).  
 [15] H.K. Avetissian, A.K. Avetissian, G.F. Mkrtchian, Kh.V. Sedrakian, Phys. Rev. E **66**, 016502 (2002).  
 [16] J.P. Verboncoeur, A.B. Langdon, N.T. Gladd, Comp. Phys. Comm. **87**, 199 (1995).